Stitching algorithm for annular subaperture interferometry

Xi Hou (侯 溪)[1,2], Fan Wu (伍 凡)[1], Li Yang (杨 力)[1], Shibin Wu (吴时彬)[1], and Qiang Chen (陈 强)[1]

[1] *Institute of Optics and Electronics, Chinese Academy of Sciences, Chengdu 610209*

[2] *Graduate School of the Chinese Academy of Sciences, Beijing 100039*

Received October 25, 2005

Annular subaperture interferometry (ASI) has been developed for low cost and flexible test of rotationally symmetric aspheric surfaces, in which accurately combining the subaperture measurement data corrupted by misalignments and noise into a complete surface figure is the key problem. By introducing the Zernike annular polynomials which are orthogonal over annulus, a method that eliminates the coupling problem in the earlier algorithm based on Zernike circle polynomials is proposed. Vector-matrix notation is used to simplify the description and calculations. The performance of this reduction method is evaluated by numerical simulation. The results prove this method with high precision and good anti-noise capability.

OCIS codes: 120.3940, 220.4840, 070.4560, 000.3870.

Subaperture interferometry has been developed to overcome the aperture size and slope sampling limitations of conventional interferometer, whose primary goal is to obtain a full-aperture map from many subaperture measurements without measuring the entire part at one time. Due to its advantages of low cost and flexibility, many researchers have explored the method and developed a variety of related techniques[1−15]. Nevertheless, the annular subaperture interferometry (ASI)[4−7] for testing large aspheric surfaces has not been developed into a commercial interferometer and applied in practical engineering. It is well known that the spatial frequency of the resulted interference pattern may be greater than the charge-coupled device (CCD) resolution when the departure between an aspheric surface under test and a spherical reference wavefront is too large. In this case, ASI has provided an alternative solution, which makes the reference wavefront with different curvature radii match the corresponding annular subaperture area of aspheric surface, then combines all subaperture data together with a suitable algorithm to get a complete surface figure. The earliest reduction method based on Zernike circle polynomials was proposed and demonstrated by Liu *et al.* in 1988[4], which can calculate full-aperture Zernike coefficients from the subaperture Zernike coefficients obtained by commercial interferogram reduction software. However, the strong coupling between the higher- and lower-order radial modes is one of the most significant problems in this method, where the coupling results from the fact that circle subapertures are used instead of annular apertures. Another reduction method with successive overlapping phase maps was presented by Melozzi *et al.* in 1993[5]. Starting from the inner phase map and subtracting the misalignment errors from its adjacent annular map, the latter is brought to coincide with the former. This process is repeated until the requested diameter, obtaining the total phase map of aspheric surfaces under test. The misalignment errors between consecutive data sets are evaluated by fitting phase data over the annular superposition regions with Zernike annular polynomials[16] owing to the orthogonal properties of such functions. Granados-Agustín *et al.* improved the method by simultaneously fitting of misalignment errors among multiple overlapping subapertures[6], which followed the idea of Otsubo[11].

However, some new challenges, particularly in the motion and algorithm components, appear when applied to large aspheric surfaces in practical engineering. Measurement accuracy has been limited by relatively poor control over errors introduced mainly by motion control component, especially for multiple overlapping subapertures. The stitching efficiency of non-overlapping subaperture configuration is higher than that of overlapping one. When the subapertures are complement, the information reflecting full-aperture aspheric surfaces will not be lost, and the number of subaperture measurements will become less. By introducing the Zernike annular polynomials[16] to solve the coupling problem, we present a modified reduction method for ASI. Our demonstration focuses on the feasibility of the method applied to testing large aspheric surfaces by use of multiple complement subaperture measurements with different misalignments and random noise.

In this letter, a concentric subaperture configuration and rotationally symmetric optical system under test are assumed. As an illustration, geometries of the three complement annular subapertures are shown in Fig. 1. The transformation between the normalized local and global coordinates can be performed by proper scaling.

By using the Gram-Schmidt orthogonalization method to Zernike circle polynomials[17], the polynomials called Zernike annular polynomials that are orthogonal over a unit annulus were developed by Mahajan[16]. The polynomials may be given as a product of a radial polynomial function $R_n^m(\rho,\varepsilon)$ and an azimuthal function. They can be written as

$$Z_n^m(\rho,\theta,\varepsilon)=\begin{cases}\left.\begin{matrix}R_n^m(\rho,\varepsilon)\cos(m\theta) & m>0\\ R_n^m(\rho,\varepsilon)\sin(|m|\,\theta) & m<0\end{matrix}\right\} & m\neq 0\\ R_n^m(\rho,\varepsilon) & m=0\end{cases}, \tag{1}$$

where the values of n and m are always integers and satisfy $m\le n$, $n-|m|$ is even, and $\varepsilon\le\rho\le 1$, $0\le\theta\le 2\pi$. Consequently, only some permissible pairs of n and m

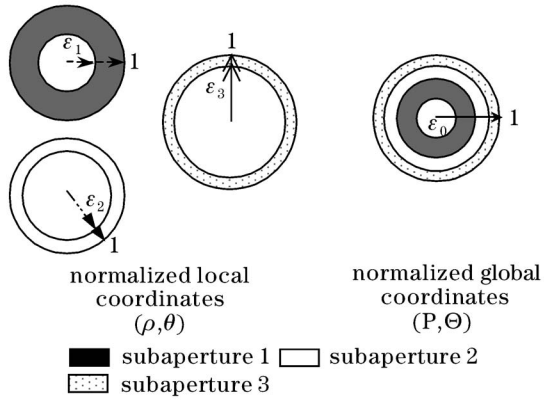

Fig. 1. Geometries of three complement annular subapertures in the normalized local and global coordinates..

exist.

Due to the complexity of recurrence definition of Zernike annular polynomials, a general symbol representation of that in a computing program was established, enabling the use of them directly and flexibly in the succulent reconstruction process. The symbolic algorithm based on Mathematica5.0[18] was provided in Ref. [19] in detail.

Then, the use of them is just like a built-in function. For example, for $\varepsilon = 0.1$, we have

$$R_1^1(\rho, 0.1) = 0.9950\rho,$$

$$R_2^0(\rho, 0.1) = -1.0202 + 2.0202\rho^2,$$

$$R_4^0(\rho, 0.1) = 1.0612 - 6.1830\rho^2 + 6.1218\rho^4, \quad (2)$$

and for $\varepsilon = 0.3$, we have

$$R_1^1(\rho, 0.3) = 0.9578\rho,$$

$$R_2^0(\rho, 0.3) = -1.1978 + 2.1978\rho^2,$$

$$R_4^0(\rho, 0.3) = 1.6521 - 7.8976\rho^2 + 7.2455\rho^4. \quad (3)$$

Based on the orthogonality of Zernike polynomials, the first 4 terms of them will be corresponding to piston, tilt in x direction, tilt in y direction, and defocus, respectively.

The full-aperture wavefront with misalignments, $W(\mathrm{P}, \Theta, \varepsilon_0)$, can be segmented into the global surface information and the local sub-aperture misalignment information in terms of the Zernike annular polynomials,

$$W(\mathrm{P}, \Theta, \varepsilon_0) = \sum_{k=1}^{K} \sum_{i=1}^{4} b_{ki} Z_{ki}(\rho_k, \theta, \varepsilon_k) + \sum_{i=5}^{L} B_i Z_i(\mathrm{P}, \Theta, \varepsilon_0), \quad (4)$$

where (P, Θ) is the normalized global coordinates, (ρ, θ) is the normalized local coordinates, ε_0 is obscuration ratio of full aperture, ε_k is obscuration ratio of the kth subaperture, K is the number of subapertures, L is the number of Zernike annular polynomials, b_{ki} is the misalignment coefficient for the kth subaperture and ith Zernike mode, and B_i is the full-aperture coefficient for the ith Zernike mode.

Based on the intrinsic relationship between full-aperture and subaperture, the full-aperture wavefront can be described as

$$W(\mathrm{P}, \Theta, \varepsilon_0) = \sum_{k=1}^{K} \sum_{i=1}^{L} a_{ki} Z_{ki}(\rho_k, \theta, \varepsilon_k), \quad (5)$$

where (ρ_k, θ) is the normalized local coordinates for kth subaperture, a_{ki} is the subaperture coefficient for the kth subaperture and ith Zernike mode.

But since the aspheric surface itself has not changed, Eq. (4) must be equivalent to Eq. (5), giving

$$\sum_{k=1}^{K} \sum_{i=1}^{L} a_{ki} Z_{ki}(\rho_k, \theta, \varepsilon_k) = \sum_{k=1}^{K} \sum_{i=1}^{4} b_{ki} Z_{ki}(\rho_k, \theta, \varepsilon_k) + \sum_{i=5}^{L} B_i Z_i(\mathrm{P}, \Theta, \varepsilon_0). \quad (6)$$

Taking the inner product of both sides of Eq. (6) with $Z_{ki'}(\rho_k, \theta, \varepsilon_k)$ $(i' = 1, 2, 3, \cdots, L)$, we have

$$\sum_{k=1}^{K} \sum_{i=1}^{L} a_{ki} \langle Z_i(\rho_k, \theta, \varepsilon_k) Z_{i'}(\rho_k, \theta, \varepsilon_k) \rangle_k = \sum_{k=1}^{K} \sum_{i=1}^{4} b_{ki} \langle Z_i(\rho_k, \theta, \varepsilon_k) Z_{i'}(\rho_k, \theta, \varepsilon_k) \rangle_k + \sum_{i=5}^{L} B_i \langle Z_i(\mathrm{P}_k, \Theta, \varepsilon_0) Z_{i'}(\rho_k, \theta, \varepsilon_k) \rangle_k, \quad (7)$$

where (P_k, Θ) is the normalized global coordinates for kth subaperture, $\langle\rangle_k$ denotes the inner product over the kth subaperture, evaluated by integration over the kth subaperture as follows

$$\langle Z_i(\rho_k, \theta, \varepsilon_k) Z_{i'}(\rho_k, \theta, \varepsilon_k) \rangle_k = \int_0^{2\pi} \int_{\varepsilon_k}^{1} Z_i(\rho, \theta, \varepsilon_k) Z_{i'}(\rho, \theta, \varepsilon_k) \rho \mathrm{d}\rho \mathrm{d}\theta, \quad (8)$$

$$\langle Z_i(\mathrm{P}_k, \Theta, \varepsilon_0) Z_{i'}(\rho_k, \theta, \varepsilon_k) \rangle_k = \int_0^{2\pi} \int_{\varepsilon_k}^{1} Z_i(\mathrm{P}_k, \Theta, \varepsilon_k) Z_{i'}(\rho, \theta, \varepsilon_k) \rho \mathrm{d}\rho \mathrm{d}\theta. \quad (9)$$

For simplicity, by use of vector-matrix notation, Eq. (7) can be rewritten as

$$[\mathbf{M}]_{KL \times KL} \mathbf{A}_{KL \times 1} = [[\mathbf{N}]_{KL \times 4K} [\mathbf{T}]_{KL \times (L-4)}] \mathbf{B}_{(4K+L-4) \times 1}. \quad (10)$$

The block diagonal matrix [**M**] is given by

$$[\mathbf{M}] = \begin{bmatrix} [\mathbf{M}_1] & 0 & \cdots & 0 & 0 \\ 0 & [\mathbf{M}_2] & \cdots & 0 & 0 \\ \vdots & \vdots & \ddots & \vdots & \vdots \\ 0 & 0 & \cdots & [\mathbf{M}_{K-1}] & 0 \\ 0 & 0 & \cdots & 0 & [\mathbf{M}_K] \end{bmatrix}, \quad (11)$$

with each block matrix $[\mathbf{M}_k]$ being a square diagonal matrix with $L \times L$ elements. The block diagonal matrix [**N**] is given by

$$[\mathbf{N}] = \begin{bmatrix} [\mathbf{N}_1] & 0 & \cdots & 0 & 0 \\ 0 & [\mathbf{N}_2] & \cdots & 0 & 0 \\ \vdots & \vdots & \ddots & \vdots & \vdots \\ 0 & 0 & \cdots & [\mathbf{N}_{K-1}] & 0 \\ 0 & 0 & \cdots & 0 & [\mathbf{N}_K] \end{bmatrix}, \quad (12)$$

with $[\mathbf{N}_k]$ being a rectangular matrix with L rows and 4 columns. The rectangular matrix [**T**] can be written as

$$[\mathbf{T}] = \begin{bmatrix} [\mathbf{T}_1] \\ [\mathbf{T}_2] \\ \vdots \\ [\mathbf{T}_K] \end{bmatrix}, \quad (13)$$

where each sub-matrix $[\mathbf{T}_k]$ contains $L \times (L-4)$ elements. By defining the row vector $\mathbf{A}_k$ as

$$\begin{aligned} \mathbf{A}_1 &= [a_{11} \quad a_{12} \quad a_{13} \quad a_{14} \quad \cdots \quad a_{1L}], \\ \mathbf{A}_2 &= [a_{21} \quad a_{22} \quad a_{23} \quad a_{24} \quad \cdots \quad a_{2L}], \\ &\vdots \\ \mathbf{A}_K &= [a_{K1} \quad a_{K2} \quad a_{K3} \quad a_{K4} \quad \cdots \quad a_{KL}], \end{aligned} \quad (14)$$

the all subaperture interferometric data are now represented by a column vector with KL elements:

$$\mathbf{A} = [\mathbf{A}_1 \quad \mathbf{A}_2 \quad \mathbf{A}_3 \quad \cdots \quad \mathbf{A}_K]^T. \quad (15)$$

We can define a column vector **B** containing all subaperture misalignment coefficients and the full-aperture surface coefficients in the global coordinates,

$$\begin{aligned} \mathbf{B} = [&b_{11} \quad b_{12} \quad b_{13} \quad b_{14} \quad b_{21} \quad b_{22} \quad b_{23} \quad b_{24} \quad \cdots \\ &b_{K1} \quad b_{K2} \quad b_{K3} \quad b_{K4} \quad B_5 \quad B_6 \quad \cdots \quad B_L]^T. \end{aligned} \quad (16)$$

In addition, we introduce the following notation:

$$[\mathbf{G}] = [[\mathbf{N}][\mathbf{T}]]. \quad (17)$$

Given the matrix [**G**], we may calculate its pseudoinverse $[\mathbf{G}]^{-1}$ by

$$\mathbf{G}^{-1} = (\mathbf{G}^T\mathbf{G})^{-1}\mathbf{G}^T. \quad (18)$$

The desired Zernike coefficients **B** describing the full-aperture wavefront are calculated by

$$\mathbf{B} = [\mathbf{G}]^{-1}[\mathbf{M}]\mathbf{A}. \quad (19)$$

Generally, the first $4K$ elements describing the subaperture misalignments in the vector **B** will be discarded. The shape of the wavefront under test is reconstructed by use of the remaining L-4 coefficients of vector **B**.

The performance of the above reduction algorithm is demonstrated by numerical simulation. Firstly, we synthesized a full-aperture wavefront map with obscuration ($\varepsilon_0 = 0.1$) by annular Zernike coefficients shown in Fig. 2(a), and generated five subaperture wavefront maps by

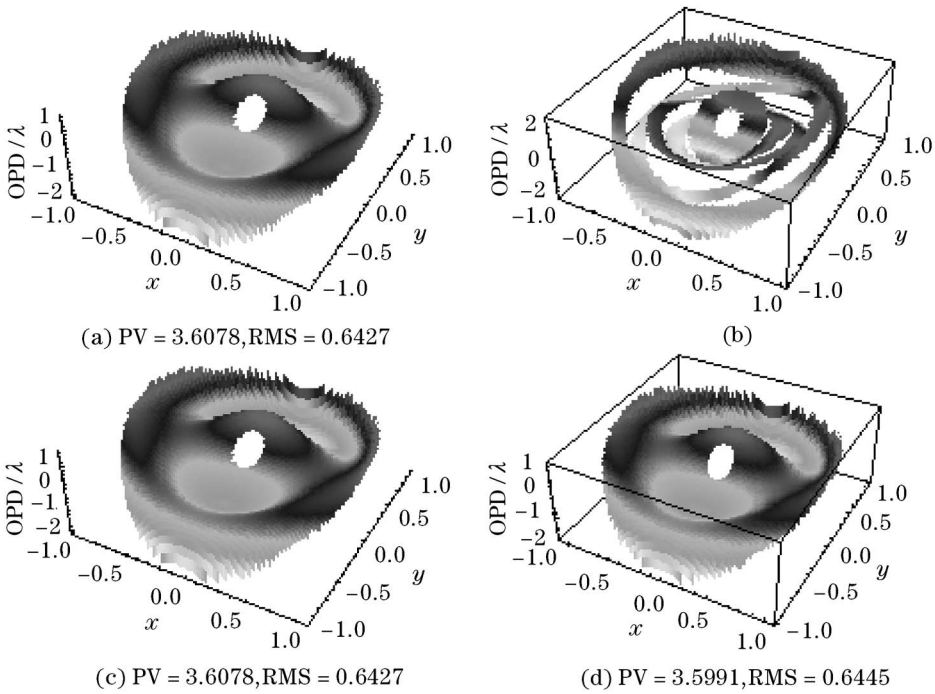

Fig. 2. Simulation results. (a) The original wavefront map; (b) isometric plot for five annular subaperture wavefronts; (c) reconstructed full-aperture wavefront map from data shown in Fig. 2(b) without random noise; (d) reconstructed full-aperture wavefront map from data shown in Fig. 2(b) with random noise $\sigma = 0.1$. OPD: optical path difference; PV: peak to valley; RMS: root mean square.

Table 1. Area and Misalignment Coefficients of Five Simulated Subapertures

Subaperture	Subaperture Area	Zernike Coefficients of Misalignments			
		Piston	x Tilt	y Tilt	Defocus
1	$0.1 \le P_1 \le 0.35$	−0.109	1.012	0.306	−0.206
2	$0.35 \le P_2 \le 0.55$	−0.043	−1.312	1.706	0.521
3	$0.55 \le P_3 \le 0.7$	0.019	−1.091	0.406	−0.206
4	$0.7 \le P_4 \le 0.85$	0.033	1.512	1.706	−0.225
5	$0.85 \le P_5 \le 1$	0.029	1.091	−0.406	0.293

Table 2. Annular Zernike Coefficients Calculated by the Proposed Reduction Algorithm

Noise-to-Signal	Annular Zernike Coefficients of Full-Aperture											
	5	6	7	8	9	10	11	12	13	14	15	16
$\sigma = 0$	−1	0	0	0	0.35	0	0	0	0	1.63	0	0
$\sigma = 0.1$	−0.998	0	−0.002	−0.007	0.376	−0.004	0.005	0.002	0.003	1.625	0.008	0.011

adding arbitrary misalignment coefficients in each subaperture area. The original full-aperture wavefront consists of -1λ primary astigmatism, 0.35λ primary spherical aberration, and 1.63λ secondary coma. The areas and misalignment coefficients of five simulated subapertures are summarized in Table 1, and the isometric plot for five annular subaperture wavefronts is shown in Fig. 2(b). For simplicity but generalization, the normalized global coordinates and 16-term Zernike annular polynomials are used in the simulation. To simulate experimental conditions in which the vibration and air fluctuations will influence inevitably the measurement results, some zero mean and Gaussian distribution random values are added to the discrete sampling points of each subaperture, where the standard deviation of random noise is σ_0.

Given a set of uniform sampling points of the original full-aperture wavefront, $\{x_1, x_2, \cdots, x_N\}$, the standard deviation S can be calculated by

$$S = \left[\frac{1}{N-1}\sum_{i=1}^{N}(x_i - \bar{x})^2\right]^{1/2}. \quad (20)$$

The noise-to-signal can be defined by

$$\sigma = \sigma_0/S. \quad (21)$$

The full-aperture Zernike coefficients calculated by the above algorithm are listed in Table 2. The original wavefront map, isometric plot of five subapertures, and reconstructed wavefront map are shown in Fig. 2. It is noted that the coefficients of the 5th, 9th, and 14th terms are close to the corresponding initial values, and the remnant coefficients are almost equal to zero. It can be seen that the proposed algorithm can reconstruct perfectly the full-aperture wavefront in the case without random noise. In such case with random noise $\sigma = 0.1$, the difference between the original and reconstructed wavefronts is extremely small. From Figs. 2(a), (c), and (d), we can clearly see that the great similarity exists between them.

In conclusion, we have developed a data reduction method for testing large aspheric surfaces with annular subaperture interferometry. For developing the method, the complex Zernike annular polynomials are represented in a computing program, and vector-matrix notation is used to simplify the description and the calculations of reduction method. The obtained numerical results demonstrate the better performance of the proposed method.

This work was supported by the National "863" Project of China. X. Hou's e-mail address is hxxh6776@sohu.com.

References

1. C.-J. Kim, Appl. Opt. **21**, 4521 (1982).
2. J. G. Thunen and O. Y. Kwon, Proc. SPIE **351,** 19 (1982).
3. J. E. Negro, Appl. Opt. **23,** 1921 (1984).
4. Y. M. Liu, G. N. Lawrence, and C. L. Koliopoulos, Appl. Opt. **27,** 4504 (1988).
5. M. Melozzi, L. Pezzati, and A. Mazzoni, Opt. Eng. **32,** 1073 (1993).
6. F. Granados-Agustín, J. F. Escobar-Romero, and A. Cornejo-Rodríguez, Opt. Rev. **11,** 82 (2004).
7. X. Hou, F. Wu, S. Wu, and Q. Chen, Proc. SPIE **5638,** 992 (2005).
8. S. C. Jensen, W. W. Chow, and G. N. Lawrence, Appl. Opt. **23,** 740 (1984).
9. C. R. De Hainaut and A. Erteza, Appl. Opt. **25,** 503 (1986).
10. G. N. Lawrence and R. D. Day, Appl. Opt. **26,** 4875 (1987).
11. M. Otsubo, K. Okada, and J. Tsujiuchi, Opt. Eng. **33,** 608 (1994).
12. T. Hänsel, A. Nickel, and A. Schindler, Proc. SPIE **4449,** 265 (2001).
13. M. Bray, Proc. SPIE **3134,** 39 (1997).
14. P. Murphy, G. Forbes, J. Fleig, P. Dumas, and M. Tricard, Opt. Photon. News **14,** (5) 38 (2003).
15. P. E. Murphy, J. Fleig, G. Forbes, and M. Tricard, Proc. SPIE **5786,** 112 (2005).
16. V. N. Mahajan, J. Opt. Soc. Am. **71,** 75 (1981).
17. J. C. Wyant, *Zernike Polynomial* (Optical Science Center, University of Arizona, Tucson, 1999) http://www.optics.arizona.edu/jcwyant/Zernikes/ZernikePolynomials.htm.
18. The Mathematica software is developed by the Wolfram Research, Inc., http://www.wolfram.com.
19. X. Hou, F. Wu, S. B. Wu, and Q. Chen, Journal of Sichuan University (Natural Science Edition) (in Chinese) **42,** 305 (2005).